RSC Advances

This is an *Accepted Manuscript*, which has been through the Royal Society of Chemistry peer review process and has been accepted for publication.

Accepted Manuscripts are published online shortly after acceptance, before technical editing, formatting and proof reading. Using this free service, authors can make their results available to the community, in citable form, before we publish the edited article. This *Accepted Manuscript* will be replaced by the edited, formatted and paginated article as soon as this is available.

You can find more information about *Accepted Manuscripts* in the **Information for Authors**.

RSC Advances

ARTICLE

Synthesis, self-assembly, and catalytic activity of histidine-based structured lipopeptides for hydrolysis reactions in water

M. Bélières[a], N. Chouini-Lalanne[a], and C. Déjugnat[a,*]

[a] Laboratoire des Interactions Moléculaires et Réactivité Chimique et Photochimique (IMRCP), UMR 5623 Université Paul Sabatier, Bât 2R1, 118, route de Narbonne, 31062 Toulouse cedex, France
* Corresponding author: *dejugnat@chimie.ups-tlse.fr*.

A new series of lipopeptides was designed to study their organocatalytic properties towards ester hydrolysis and the role of their self-assembled structures on the catalysis. Synthesis of the catalysts was achieved by grafting fatty chains on tripeptides either at the C-terminal position or at the N-terminal extremity, affording amphiphilic character and self-assembling properties. Insertion of a histidine in the peptide sequence was chosen to bring the organocatalytic activity. Self-organization was evidenced first by the determination of critical aggregation concentrations and then by characterizing the aggregates formed performing scattering techniques and microscopy. Variation of the structures (peptide sequence, hydrophobic character) led to the formation of various aggregates, from globular objects to fibers. All derivatives containing histidine presented a catalytic activity on the hydrolysis reaction of *p*-nitrophenyl acetate in aqueous solution. The influence of the self-organization on the catalysis was evidenced by showing different behaviors observed between monomers and aggregates.

Introduction

While organometallic catalysts and enzymes have been dominating the field of catalysis for a long time, organocatalysis appears as an alternative approach with a fast growing interest. Organocatalysts are metal-free small organic molecules which are usually stable, nontoxic, not expensive, easily accessible, and recyclable.[1-5] Among them are amino-acids and peptides (inspired from natural enzymatic catalytic sites),[6-10] which are most of the time used in organic solvents while water might be involved and play a major role in some mechanisms.[11] Another type of catalysis can also be observed in aqueous medium: an interfacial catalysis can be brought thanks to the ability of self-assembled aggregates (mostly micelles, but also vesicles formed by amphiphiles) to increase reactions rates.[12-19]

In this context, we have chosen to combine organocatalysis and interfacial catalysis by considering the use of self-assembled amphiphilic lipopeptides as catalysts in water (supramolecular enzyme mimics).[20] Thanks to the combination of various weak interactions (electrostatics, H-bonding, hydrophobic effect, etc.), lipopeptides and surfactant-like peptides have remarkable aggregation properties that lead to the formation of various self-organized systems.[21-28] Moreover these aggregates could present an organocatalytic activity, for example in the case of an aldol reaction catalyzed by a proline-based, gel-forming peptide.[29, 30] In addition, the supramolecular organization can affect the catalytic properties,[31-33] showing that there might be an interplay between aggregation and catalysis.

In the present study, we have chosen to focus on hydrolysis as this reaction plays a major role in many biological processes such as digestion of proteins by proteases, metabolism of esters and lipids involving lipases, or degradation of phosphoesters (regulation of inorganic phosphate, hydrolysis of ATP or nucleic acids, etc.). Moreover the control of this model reaction could find applications in various field such as enzyme inhibition,[34] molecular biology, or genetic engineering. In a bio-inspired approach, looking at the active sites in hydrolases reveals that histidine plays a major role in the catalytic activity of the enzymes.[35] Therefore we have considered histidine-based lipopeptides as potential self-assembled organocatalysts for hydrolysis reactions in water. Indeed hydrolysis catalyzed by histidine-related compounds is widely documented in the case of

simple esters,[36-42] phosphoesters,[43-52] or even DNA.[53, 54] As a first step we initiated this study considering the widely used ester (*p*-nitrophenyl acetate) as model substrate.

In a first part we describe the design and the synthesis of a series of potentially catalytic amphiphilic lipopeptides. The tripeptide sequences contain a histidine at the terminal position to provide catalytic activity or they are based on triglycine to afford non-reactive control derivatives. Moreover the modulation of the alkyl chain allows control over the self-assembly properties. In a second part we present the self-assembling properties of the lipopeptides, including determination of critical aggregation concentrations and characterization of the aggregates by microscopy and scattering techniques. In the third and final section, we present the catalytic activity of the lipopeptides on the hydrolysis of the model ester *p*-nitrophenyl acetate. The aim is to evidence the respective contributions of organocatalysis (due to the presence of histidine) and interfacial catalysis (due to self-assembly).

Results and discussion

Design and synthesis of lipopeptides

The amphiphilic structures we have considered are generally composed of a tripeptide linked to a fatty hydrocarbon chain. The choice of a triad as the polar head group was motivated by the wish to later get access to more functional structures by the incorporation of different aminoacids, while keeping a short sequence remaining easy to handle. As a starting point we have decided to use histidine at the extremity of the surfactants, using two simple glycines as linkers between histidine and the fatty chain. Few similar structures have already been described in patented studies on gel formation and on hair growth formulations, showing the potential self-assembling and bio-compatible properties of this kind of derivatives.[55-57] As controls, lipopeptides based on triglycine were also synthesized. These molecules do not contain histidine and are supposed to have no organocatalytic activity while keeping self-assembling properties.[58] Depending on the grafting side, N-terminal or C-terminal peptides were obtained. In addition, the hydrophobicity of the surfactants has been modulated by varying the alkyl chain length from octyl to dodecyl. Moreover two other C-terminal structures were considered: the first one contained a terminal histidine but the carboxylic function was blocked as a methyl ester; the other one contained also a terminal histidine but a serine was included instead of the central glycine of the triad. Indeed this amino acid is frequently present in catalytic triads of numerous hydrolytic enzymes such as proteases, lipases, etc.[59] Finally a catanionic peptide was obtained by proton exchange between a C-terminal peptide and its N-terminal analogue *via* a simple acid-base reaction.[60]

The lipopeptides were obtained in good yields by classical solution synthesis based on Boc strategy and DIC/OxymaPure® activation.[61] This choice allowed us to produce the peptides in a greener way than conventional methods, reducing notably the use of toxic solvents (such as DMF) or potentially explosive reactives (such as HOBt). This approach lies in the field of Green Chemistry which has emerged as a powerful tool to reduce human imprint on environment and to develop safer processes.[62-64] Among its twelve principles are the molecular economy, the use of natural resources and safe solvents (water), and catalysis. These notions are here combined by considering organocatalysis in aqueous solutions and based on natural renewable substances. General protocols are reported in the experimental part while full spectroscopic analysis can be found in the *Supporting Information*. The structures of the lipopeptides are reported in Figure 1.
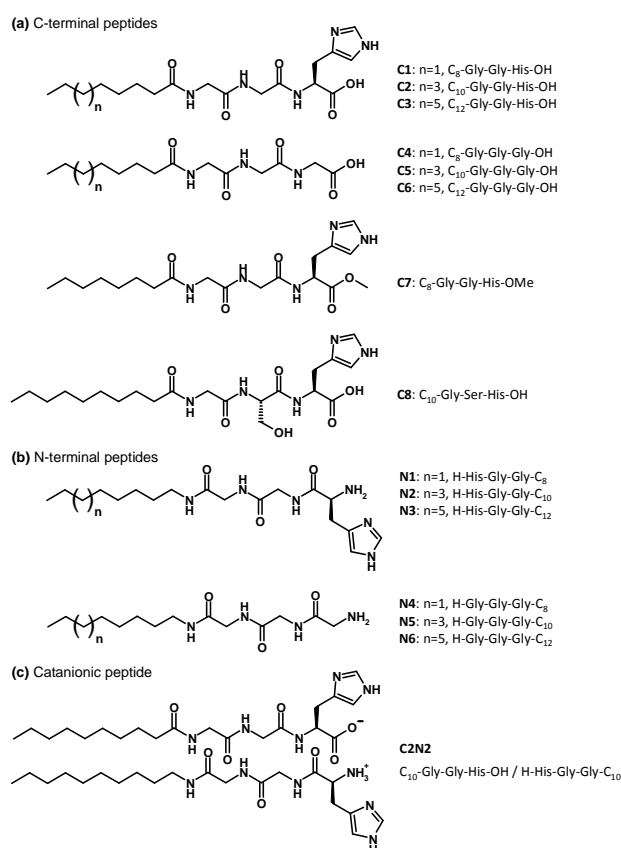

Figure 1. Structures of the lipopeptides studied: (a) C-terminal peptides, (b) N-terminal peptides, and (c) catanionic peptide.

Physico-chemical properties and self-assembly

Lipopeptides are intrinsically amphiphilic and such molecules can self-assemble in a large variety of more or less ordered structures at the solid state or in aqueous solutions. Upon self-organization, the structures obtained can vary from what predicted for classical surfactants because of the additional specific structuration of peptides *via* H-bonding and other weak interactions between the lateral chains of the aminoacids.[23, 28] At the solid state, FT-IR spectroscopy can bring information on the secondary structures of the peptides by analyzing the amide I-III bands positions in the range 1700-1200 cm^{-1}.[65, 66] For all lipopeptides, the amide I band lied at 1645-1652 cm^{-1} while the amide II band was observed at 1544-1554 cm^{-1} (full spectra are

reported in the *Supporting Information*). This suggest that the peptide sequences adopt a random or random coil conformation,[65, 66] which is not surprising regarding the shortness of the sequences.

Dissolution of the lipopeptides in aqueous buffered solutions (50 mM HEPES buffer, pH = 7) generally produced opalescent fluids, ranging from slightly cloudy/bluish to strongly opaque solutions. This already shows that the lipopeptides self-assembled in quite large aggregates (>100 nm) because usually micellar solutions remain limpid.

In aqueous solutions, surface tension measurements were performed as a function of the lipopeptides' concentrations to determine the critical aggregation concentrations (CACs). Generally upon increasing concentration, surface tension decreases then reaches a plateau at a threshold concentration value that corresponds to the CAC.[67] As an illustrative example, measurements performed for lipopeptides C1 to C6 are shown in Figure 2 (full measurements are reported in the *Supporting Information*).
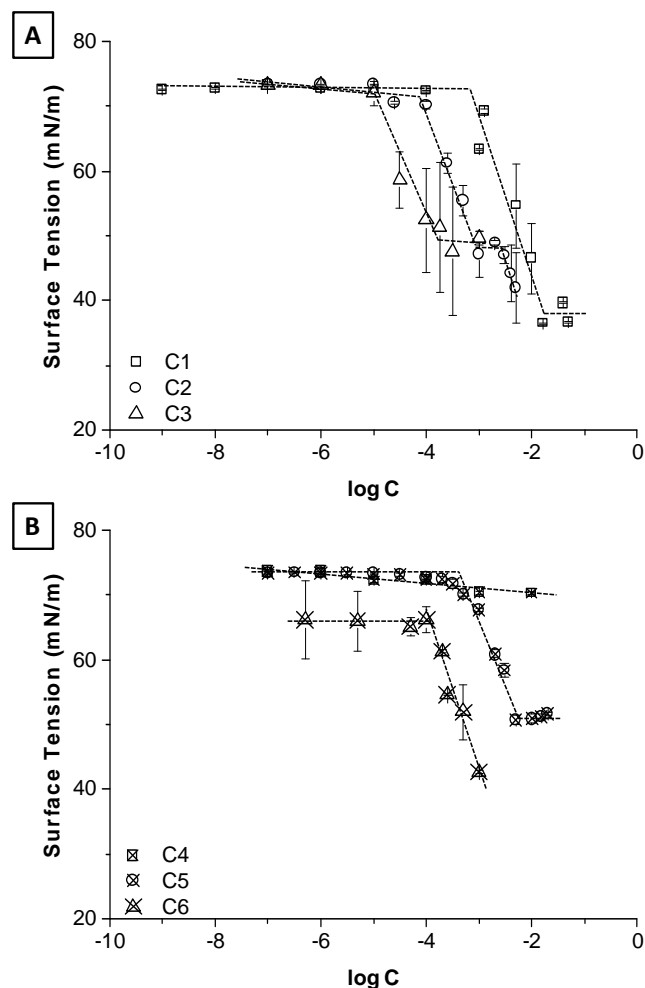

Figure 2. Variation of the surface tension as a function of the concentration for lipopeptides C1 to C3 (A) and C4 to C6 (B).

Another complementary technique based on pyrene fluorescence was also used to determine the CACs,[68, 69] especially for lipopeptides presenting high CACs. Both techniques (tensiometry and pyrene fluorescence) were performed in parallel on most of the lipopeptides, giving CAC values of the same order, and showing that they were in rather good agreement (full results can be found in the *Supporting Information*). From these two techniques, averaged CACs were obtained; the accuracy was at best 20 %. Full results are reported in Table 1.

Table 1. Critical aggregation concentrations (CACs) of the lipopeptides determined from tensiometry and fluorimetry.

Lipopeptide	CAC (mM) from tensiometry	CAC (mM) from fluorimetry	average CAC (mM)	γ_{CAC} (mN/m)
C1 (C_8-GGH-OH)	10 ± 2	16.3 ± 3.3	13 ± 4	38 ± 2
C2 (C_{10}-GGH-OH)	1.3 ± 0.3	0.75 ± 0.15	1.0 ± 0.5	45 ± 2
C3 (C_{12}-GGH-OH)	0.25 ± 0.05	0.33 ± 0.08	0.3 ± 0.1	49 ± 2
C4 (C_8-GGG-OH)	no CAC [a]	no CAC [a]	no CAC	-
C5 (C_{10}-GGG-OH)	5 ± 1	5.4 ± 1.1	5 ± 1	51 ± 2
C6 (C_{12}-GGG-OH)	1.0 ± 0.3	0.85 ± 0.17	0.9 ± 0.3	43 ± 2
C7 (C_8-GGH-OMe)	no CAC [a]	no CAC [a]	no CAC	-
C8 (C_{10}-GSH-OH)	0.10 ± 0.03 and 2 ± 1 [b]	4.0 ± 0.8	3 ± 1	39 ± 2
N1 (H-HGG-C_8)	not measured	16 ± 5	16 ± 5	-
N2 (H-HGG-C_{10})	0.7 ± 0.1	1.4 ± 0.3	1.1 ± 0.4	37 ± 2
N3 (H-HGG-C_{12})	not measured	0.10 ± 0.02	0.10 ± 0.02	-
N4 (H-GGG-C_8)	1.8 ± 0.6 [c]	4.7 ± 0.9	3.2 ± 1.5	55 ± 2
N5 (H-GGG-C_{10})	0.4 ± 0.1 [c]	no CAC [a]	no CAC	52 ± 2
N6 (H-GGG-C_{12})	1.0 ± 0.3 [c]	no CAC [a]	no CAC	52 ± 2
C2N2	0.5 ± 0.1	0.4 ± 0.1	0.5 ± 0.1	42 ± 2

[a] no CAC was detected upon increasing concentrations till the solubility limit
[b] two "CACs" were observed; at the first one, the surface tension only dropped to 53 mN/m meaning that this transition might refer to a pre-organization (oligomerization) rather than to a true formation of aggregates
[c] as in the case of C8, the surface tension only decreased to about 55 mN/m referring probably to a pre-organization

In parallel, dynamic light scattering (DLS) was used to estimate the size of the aggregates formed by the lipopeptides above their CACs. However, only few peptides gave valuable results using this technique. The hydrodynamic diameters, measured just above the CACs (solutions became turbid upon

slight increase of the concentrations) were 300-500 nm for C1, 250-350 nm for C2, and 200 nm for N1. These sizes cannot correspond to micelles and they could rather refer to larger aggregates, such as vesicles, pieces of membranes, fibers, etc. Besides these three lipopeptides, limited solubilities prevented accurate DLS measurements. In fact for most of the peptides, precipitation (or gel formation) occurred at concentrations just above the CACs values. So in that cases it was not possible to prepare samples being concentrated enough to allow relevant DLS analysis.

In the C-terminal series (C1 to C6) we observed that the peptides were weakly surface active (surface tensions only decreased from 72 to about 40 mN/m). As in the case of classical surfactants, increasing the alkyl chain length led to a decrease of the CACs due to favored hydrophobic interactions.[67] Moreover, replacing histidine by glycine led to a global four-time increase of the CACs, meaning that the presence of histidine in the C-terminal lipopeptides favored the self-assembly. This could be explained either by stabilizing π-stacking interactions between imidazole rings, or by a global charge compensation decreasing electrostatic repulsions between polar head groups (assuming that negatively charged carboxylates stand at the extremity of the molecules, while some imidazole rings are positively charged at pH = 7). pKa determinations were realized for some lipopeptides at 2 mM by acid-base titrations and by analysis based on second-derivative plots (see *Supporting Information*) to evidence the role of electrostatic interactions. At pH = 7, C-terminal functions are fully deprotonated and exist as carboxylates. pKa values of the imidazole rings were found to be 7.1 ± 0.1 for C1 and C2 indicating that half of the rings became protonated. Therefore these positive charges could partially compensate the repulsions between carboxylates and favor aggregation. Moreover aggregation had no significant influence on the pKa values (at 2 mM C1 exists as monomers while C2 is aggregated). This could suggest that the imidazole rings were not directly implied in the aggregation process.

In the case of C7, the presence of an ester function (not charged) dramatically reduced the solubility and the peptide precipitated before any CAC could be measured. Finally replacement of the central glycine by a serine (compound C8) increased the CAC by a factor of 3 as compared to C2. This might be due to unfavorable steric hindrance, even though C8 seems to form pre-aggregates at very low concentration. Indeed a first "CAC" could be detected by tensiometry at 0.1 mM, indicating that the alcohol function in C8 first favors a kind of oligomerization, probably thanks to the formation of H-bonds between the lipopeptides. This pre-organization was not observed with fluorescence measurements, reinforcing the hypothesis that there is an intermediate state, possibly made of hydrated oligomers, before a more significant self-assembly occurs. Moreover hydrogels were easily obtained from solutions of C8, supporting the idea of H-bond networks at higher concentrations.[70]

In the N-terminal series we observed that the peptides N1 to N3 were more surface active than their analogs of the C-terminal series (surface tensions decreased from 72 to about 30 mN/m).

Regarding the effect of the alkyl chain length, increasing the hydrocarbon part from N1 to N3 led to a strong decrease of the CAC values, which were divided by a factor of 10 for each addition of two methylene groups in the chain.). In contrast, peptides N4 to N6 were very weakly surface active (surface tensions only dropped to about 52-55 mN/m) and no clear aggregate formation could be evidenced. Like in the case of the C-terminal series, this indicates that the triglycine sequence is much less efficient in promoting aggregation than in the case of a histidine-containing triad.

Finally the catanionic lipopeptide C2N2 self-assembled at concentrations lower than what observed for its parent lipopeptides C2 and N2. This is a typical behavior, the aggregation being favored both by charge compensation and hydrophobic interactions between the fatty chains.

In order to visualize the aggregates formed by the lipopeptides, transmission electron microscopy (TEM) was performed on aqueous solutions above the CACs. While N1 clearly formed "hairy" spherical aggregates whose diameters corresponded to DLS data (Figure 3A), other lipopeptides readily self-assembled in more or less complex fibrillar aggregates. For example, N2 produced pearl necklace structures with spherical objects (50-100 nm in diameter) distributed along the fibers (Figure 3B). With C2, twisted fibers were observed (Figure 3C) while C2N2 produced networks of fibers including few smaller roughly spherical objects (Figure 3D).
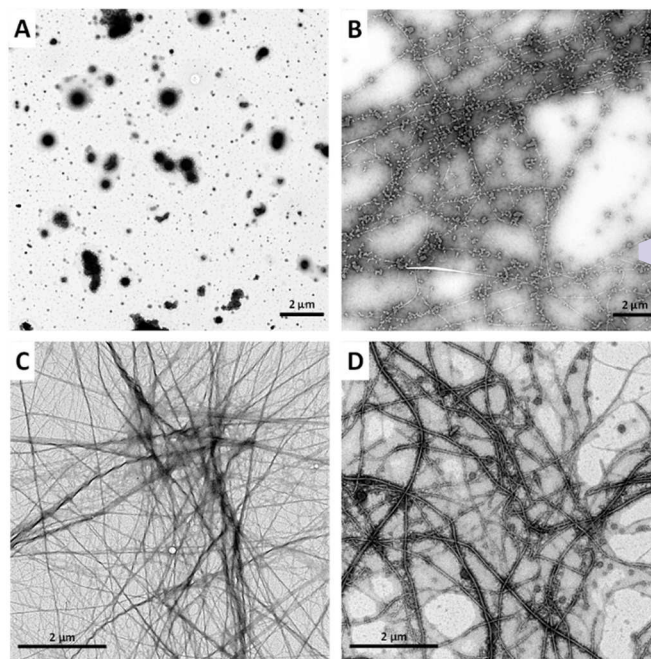

Figure 3. Transmission electron micrographs showing the aggregates formed by lipopeptides N1 (A), N2 (B), C2 (C), and the catanionic derivative C2N2 (D).

These observations are globally consistent with the visual appearance of the lipopeptides solutions which were opalescent or even milky above the CACs, some of them even leading to the formation of hydrogels. Moreover, the variety of the objects

formed shows that the aggregation is very dependent both on the peptidic sequence and on the alkyl chain lengths. This property is very important and allows modulating supramolecular aggregates by a fine tuning of the lipopeptides' chemical structure, which could be of special interest when studying the role played by interfaces and dynamics on the catalytic properties of these systems.

Finally, preliminary small-angle neutron scattering experiments (SANS) were conducted on peptides C1 and N1 to get more insights on the structural characteristics of the aggregates (only these samples were measured, because the concentrations of the other peptides were too low – due to weak solubility – to allow accurate measurements). The intensity of the signal I(Q) was corrected for the contribution of the solvent and for the incoherent scattering, and it was finally normalized to obtain values in absolute units. SANS patterns are reported in Figure 4.
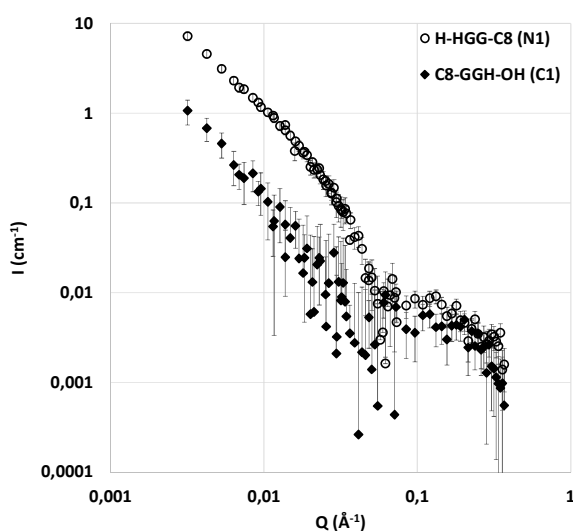

Figure 4. Experimental SANS signals I(Q) for lipopeptides N1 (16 mM) and C1 (20 mM) in phosphate buffer at pH = 7 and at 25 °C (solvent was D_2O).

First, we observe that the scattering profiles correspond to relatively large objects since the Guinier regime is not visible even at the lowest Q values ($3 \cdot 10^{-3}$ Å^{-1}). We deduce that the gyration radii R_g of the aggregates are limited by $1/R_g < 3 \cdot 10^{-3}$ Å^{-1} leading to $R_g > 350$ Å, a size which is too high for micellar aggregates. Then it appears that both lipopeptides presented similar SANS profiles, indicating that the same kinds of objects are present in solution. At low Q values, we observe a variation of the intensity following a Q^{-2} decrease, which suggests the presence of sheet-like structures or vesicles (the membrane thickness remaining very small compared to the sphere radius).[71] This is consistent with the observation of globular hairy aggregates formed by N1 and imaged by TEM. Moreover, both patterns presented a Bragg peak centered at $Q_0 = 0.12$ Å^{-1} corresponding to an inter-lamellar distance d (or bilayer spacing) of $d = 2\pi/Q_0 = 52$ Å. These preliminary measurements conducted on the shortest (and less hydrophobic) lipopeptides N1 and C1 are then consistent with the formation of globular systems which

remained stable for several days before SANS analysis. It is interesting to note that even slightly more hydrophobic peptides self-organize into fibrillar structures rather than globules. We can assume that the fibers might represent the most stable and final aggregates formed by the lipopeptides after the initial transient formation of globular objects. This could be related to the mechanism described for the formation of amyloid fibers, in which small aggregates are first originally formed before their gradual transformation into larger fibrillar structures upon aging.[72, 73]

Catalytic activity on model ester hydrolysis: kinetics experiments

Description of the system used

We have shown in the previous paragraph that the lipopeptides are able to self-assemble in aqueous solutions leading to various structures. In this section we aim at evidencing whenever these peptides could act as catalysts for hydrolysis reactions, and what could be the influence of self-organization on such a catalysis. As a first step we have considered the ester *p*-nitrophenylacetate (pNPA) as a model substrate. Indeed the hydrolysis of pNPA is easily monitored by UV-Vis spectroscopy thanks to the formation of the highly colored product *p*-nitrophenolate (pNP, yellow).[74] Hydrolysis experiments were carried out in the same conditions as for the characterization of lipopeptides' self-assembly (buffered solutions, pH = 7). Thus the extinction coefficient of pNP was determined in HEPES buffer at pH = 7. A global value of 7772 L·mol^{-1}·cm^{-1} at 406 nm was determined in solution for both co-existing phenolate ion and p-nitrophenol (pKa = 7.15), while phenolate remained the only absorbing specie at this wavelength. The hydrolysis reaction is shown in Figure 5.
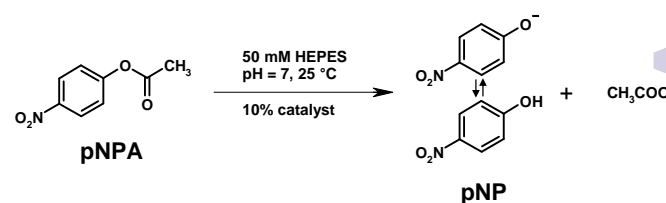

Figure 5. Hydrolysis reaction of pNPA in aqueous solution containing 10 % catalyst, and leading to the formation of pNP and acetate.

Often considered in the literature as a reference, histidine was chosen as a model catalyst.[37] Moreover we have chosen to maintain the amount of catalysts at 10 %, which remains a reasonable (or even low) ratio in various peptide-based organocatalysis studies.[38, 75-77] The first experiment was to check the catalytic activity of histidine. Starting with an initial pNPA concentration $[pNPA]_0 = 20$ mM, we could observe a linear increase of the absorbance at 406 nm as a function of time, related to the formation of pNP. In the presence of 10 % histidine ([His] = 2 mM), the conversion was 6 % after 2 h with an initial rate of $v_{0,His} = 106 \cdot 10^{-7}$ mol.L^{-1}.min^{-1}. These values were much higher than for the control experiment, in the absence of catalyst (buffer alone: conversion = 0.5 %, $v_{0,buffer} = 7 \cdot 10^{-7}$ mol.L^{-1}.min^{-1}) and this justified the choice of histidine as a reference catalyst.

Then we have studied the catalytic activity of our compounds towards pNPA hydrolysis, and compared the results with those obtained with histidine and control triads, namely Ac-GGH-OH and H-HGG-NHMe bearing only one methyl group as alkyl chain, on the C-terminal and N-terminal positions, respectively. In all cases, the ratio [catalyst]/[pNPA] was kept constant and equal to 10 %. The choice of the catalysts concentrations was driven by the self-organization properties of the lipopeptides as well as by the solubility of pNPA. Regarding the choice of the concentration to study the hydrolysis in the aggregated state, two limitations occurred. On one hand, lipopeptides bearing C_{12} alkyl chains were only scarcely soluble above the CAC and formed very turbid solutions even at 1 mM, making difficult the UV-Vis monitoring due to light scattering. On the other hand, lipopeptides bearing C_8 alkyl chains and presenting very high CACs would have required working with up to 0.1 M pNPA solutions which would have also led to turbid suspensions due to the limited solubility of the substrate in water. Therefore we decided to focus on lipopeptides bearing C_{10} alkyl chains, because all of them presented aggregated states at 2 mM and pNPA was soluble enough in HEPES buffer at 20 mM. In parallel, analogous lipopeptides bearing C_8 alkyl chains were considered to study the monomeric states, because all of them presented CACs values much higher than 2 mM.

Results

pNPA conversion was measured as a function of time for 2 h by monitoring the appearance of pNP, as calculated by: conversion = (Absorbance/ε_{pNP})/[pNPA]$_0$. Full results are reported in Figure 6. In addition, the initial rates of the reactions and the conversion ratios after 2 h are reported in the table 2.

Table 2. Initial rates of the hydrolysis reaction of pNPA ([pNPA]$_0$ = 0.02 mol.L^{-1}) in the presence of different catalysts (10 % mol) in 50 mM HEPES buffer (pH = 7, 25 °C), and the corresponding conversion ratio after 2 h.

| Catalyst	Aggregation state	v_0 (10^{-7} mol.L^{-1}.min^{-1})	Conversion at 2h (%)
no catalyst	-	7 ± 3	0.5 ± 0.2
histidine	monomers	106 ± 8	6.4 ± 0.5
C_{10}-GGG-OH	monomers	10 ± 2	0.6 ± 0.4
H-GGG-C_{10}	monomers	9 ± 4	0.5 ± 0.2
C_{10}-GGH-OH	aggregates	314 ± 19	7.4 ± 0.3
C_8-GGH-OH	monomers	311 ± 4	8.2 ± 0.5
Ac-GGH-OH	monomers	242 ± 50	6.9 ± 0.3
C_{10}-GSH-OH	aggregates	343 ± 44	7.5 ± 0.4
H-HGG-C_{10}	aggregates	124 ± 3	6.4 ± 0.2
H-HGG-C_8	monomers	173 ± 4	8.0 ± 0.1
H-HGG-NHMe	monomers	91 ± 21	4.5 ± 0.5
C_{10} catanionic (C2N2)	aggregates	220 ± 12	6.9 ± 0.3
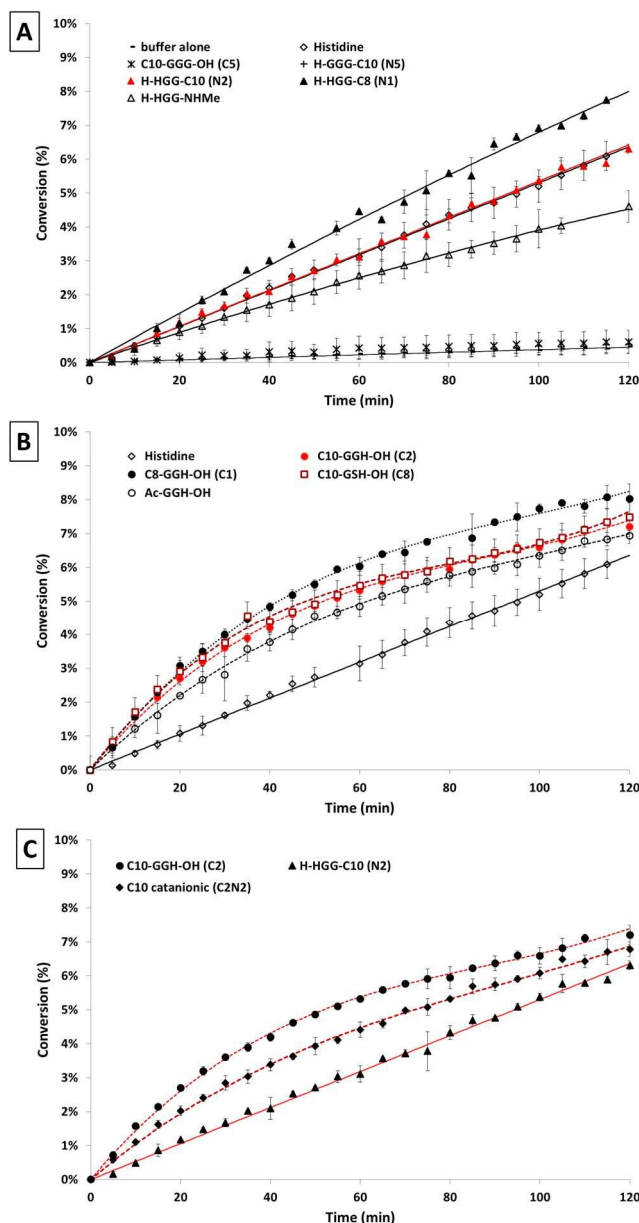
Figure 6. Evolution of pNPA conversion into pNP as a function of time, in the presence of 10 % catalysts (HEPES buffer, pH = 7, 25 °C). (A) N-terminal peptides, triglycine-based controls, histidine, and buffer alone. (B) C-terminal peptides and histidine. (C) Catanionic lipopeptide C2N2 and the parent lipopeptides C2 and N2. Lines and dashed lines are drawn as eye guides. Red curves refer to aggregated systems.

In the absence of peptidic catalysts (buffer alone, Figure 6A), the hydrolysis reaction was very slow and the kinetics profile was linear, as stated above. Analysis of kinetic parameters is reported in the *Supporting Information*. It shows that the reaction is of first order with respect to the substrate and that hydrolysis undergoes a general acid-base catalysis mainly mediated by the basic form of HEPES. It implies that any weak acids or weak bases that would be added to the medium could also act as catalysts.

Using triglycine-based lipopeptides as catalysts (either C5 or N5) led to results close to those obtained with the buffer alone (Figure 6A). These experiments show that C5 and N5 do not present any apparent catalytic activity, and support first the idea that the presence of histidine in the peptidic sequence is a pre-requisite to confer such an organocatalytic property. The introduction of weak acids or bases (ammonium for N5, carboxylate for C5) is not sufficient to enhance the global buffer catalytic activity. Moreover supramolecular catalysis is not evidenced here because the concentrations of the lipopeptides were below their respective CACs.

Using lipopeptides containing histidine either at the C-terminal position (C1 and C2) or at the N-terminal position (N1 and N2), or in the catanionic combination C2N2 led to different results. For each compound the catalytic activity was evidenced and found to be equal or superior to that of simple histidine.

In the N-terminal series, N1 (monomeric state) was found to be about twice more efficient as the reference triad H-HGG-NHMe containing a simple methyl group as alkyl chain and which presented a linear profile of hydrolysis (Figure 6A). This shows that the addition of a hydrophobic character to the catalyst, thanks to the presence of the alkyl chain, promotes the catalytic activity towards hydrolysis. It suggests that the hydrophobic fatty chain interacts in a positive way with the quite hydrophobic substrate pNPA, making it closer to the histidine-containing catalytic group and enhancing therefore the hydrolysis efficiency. Then, moving from N1 (monomeric state) to N2 (aggregated state) led to a slight decrease of the organocatalytic efficiency which then reached the level observed with single histidine. The hydrolysis profile of N2 was also linear and lied between those of N1 and the reference triad. Therefore in this series, the aggregates appear as less efficient catalysts than the monomers. This observation could be at a first look quite surprising because aggregates such as micelles usually exhibit enhanced catalytic activity thanks to the formation of a dynamic interfacial zone where the reactants are in closer contact compared to the bulk. In our case we have shown that the substrate pNPA seems to have a pronounced affinity with the hydrophobic alkyl chains; moreover the aggregates formed by N2 are not micelles but rather much less dynamic fiber-like objects. Therefore it looks like the substrate is retained in the hydrophobic region of the aggregates and could not access the hydrolytic nucleophiles as easily as in the case of N1. This phenomenon has recently been reported for redox-controllable self-assembling peptides for which catalytic activity in the hydrolysis of ester was much higher in the case of dynamic micelles rather than for fibers.[78]   This protecting effect could be of special interest for example in the formulation of active esters that should be slowly released in a controlled way. We show here that a fine tuning of the structures of the catalytic lipopeptides allows the control of the aggregation and makes possible the direction of the catalysis efficiency towards either an enhanced activity (active monomers) or a reduced one (protective aggregates).

In the C-terminal series (Figure 6B), some differences appeared compared to the N-terminal series. First the hydrolytic profiles were not linear anymore, suggesting different and/or more complex mechanisms. After an initial burst with initial rates being 2-3 times higher than for corresponding N-terminal catalysts, the hydrolysis slowed down significantly so that the conversion ratios after 2 h reactions were similar to that observed with N-terminal catalysts. The C-terminal lipopeptides appear initially to be more efficient catalysts that rapidly seem to get partially saturated, as in the case of enzymatic catalysis. Like in the case of N1 and N2, aggregation of the catalyst decreased the apparent catalytic activity: the lipopeptide C1 (monomeric state) was the most efficient catalyst, whereas the catalytic activity was reduced for C2 (aggregated state), which dropped to a level just above the one of the reference triad Ac-GGH-OH. Again this evidences the subtle balance that should be managed regarding the hydrophobic part of the catalysts, either to produce active, non-aggregated species or rather protective, aggregated objects. Still in the C-terminal series, the introduction of a serine in the middle of the peptidic sequence (comparing C2 and C8) did not changed significantly the catalytic activity. This shows that the potential supporting role played by serine in the hydrolysis mechanism has to be relayed by another catalytic amino-acid (such as aspartic acid) as evidenced in many catalytic triads of hydrolases.[79]

In the case of the catanionic derivative C2N2 (Figure 6C), the catalytic activity was found to be exactly the average of activities independently observed with C2 and N2 respectively. Although a synergistic effect had been evidenced in the aggregation behavior (lower CAC), here the system simply behaves as a simple combination of the isolated components. In fact we have shown that the aggregates formed by C2N2 are not radically different from the aggregates formed by C2 or N2. This means that, from a supramolecular point of view, combining C2 and N2 did not bring any additional feature that could have promoted the interfacial catalysis. Therefore, from a molecular point of view, the catanionic association is equivalent to the simple combination of the chemical moieties implied in the organocatalytic process.

Conclusions

In this paper we have presented the synthesis of surface active, histidine-based lipopeptides as well as their aggregation properties and their catalytic activity for hydrolysis reactions. The controlled synthesis of the catalysts gave access to a series of various compounds bearing an alkyl chain grafted to a tripeptide sequence, either at the C-terminal position or at the N-terminal position. The peptide sequences potentially included histidine to bring organocatalytic properties. In addition, the control of the chain length allowed the tuning of the hydrophobicity of the lipopeptides with a view to vary their supramolecular properties. Determination of the critical aggregation concentrations showed that the synthesized derivatives could self-assemble in water. Indeed the catalysts formed aggregates in aqueous solution, which were characterized by scattering experiments (light, neutrons) and electron microscopy. The large, non-dynamic aggregates ranged

from globular objects (for the most hydrophilic compounds) to fibrillar structures. These assemblies were then tested as catalysts for the hydrolysis of a model substrate (para-nitrophenyl acetate) and the catalytic activity was compared to the one observed with control derivatives or non-aggregated lipopeptides. The main results of these preliminary catalysis experiments are: *(i)* histidine should be included in the peptide sequence to get catalytic activity; *(ii)* different mechanisms are evidenced regarding the use of C-terminal or N-terminal peptides; *(iii)* lipopeptides are more efficient catalysts as monomers than in aggregates showing that a subtle balance of the hydrophobic part could be used to orientate towards activated hydrolysis or rather protection of the substrate.

Globally these results show that the control of the catalyst's chemical structure allows the tuning of the self-assembling properties, which themselves could guide the catalytic activities. Further experiments are under progress to explicit the different mechanisms implied in these reactions (especially between the C- and N-terminal series) and to determine the quantitative contributions of the different tunable parameters (charges, position of histidine, hydrophobic interactions, etc.). In addition the hydrolytic activity of these new self-assembling organocatalysts will be extended to other substrates of interest, like biologically active esters, phosphate esters, and even biomacromolecules such as DNA.

Acknowledgements

Experimental part

Materials and synthesis

Lipopeptides C2, C8, and N2 were obtained from Genscript (Hong Kong) while the other molecules were synthesized by classical solution synthesis based on Boc strategy and DIC/OxymaPure® activation (see below). H-Gly-Gly-OH, Boc-Gly-Gly-OH, H-His(1-Trt)-OMe.HCl, and Boc-His(1-Boc)-OSu were obtained from Bachem and H-Gly-Gly-Gly-OH from Abcr. Octanoyl chloride, decanoyl chloride, dodecanoyl chloride, octylamine, and dodecylamine were purchased from Sigma-Aldrich (France) and decylamine from Abcr. Triisopropylsilane (TIS), Oxyma and diisopropylcarbodiimide (DIC) were obtained from Sigma-Aldrich while diisopropylethylamine (DIEA) and trifluoroacetic acid (TFA) were from Abcr and VWR respectively. Tert-butyl methyl ether (TBME) was provided by Alfa Aesar and dichloromethane (DCM), ethyl acetate (EtOAc), methanol (MeOH) were from Sigma-Aldrich. Other compounds included acetic acid (AcOH) from Sigma-Aldrich, sodium

chloride (NaCl) from Abcr, sodium hydrogencarbonate (NaHCO$_3$) and anhydrous sodium sulfate (Na$_2$SO$_4$) from Carlo Erba Reagents. Water used in all experiments was produced by a two-stage Milli-Q filtration system from Millipore and had a resistivity higher than 18.2 MΩ·cm.

Except for C2, C8, and N2, the lipopeptides were synthesized in solution using Boc strategy and DIC/Oxyma® activation.

Lipopeptides C1 and C3 were synthesized according to the following general sequence depicted in Figure 7.
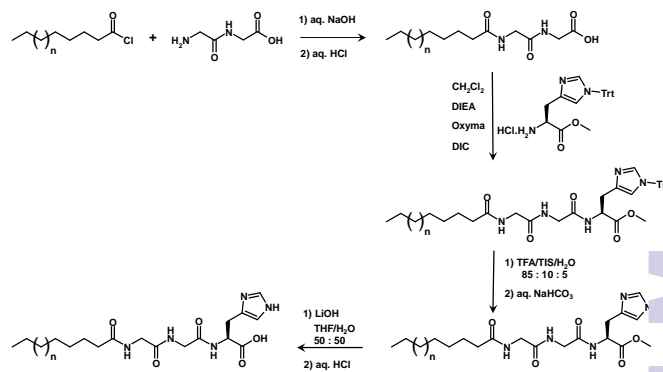

Figure 7. General synthetic pathway for the preparation of lipopeptides **C1** and **C3**.

C$_n$-Gly-Gly-OH. Acylated diglycines were obtained by a Schotten-Baumann reaction in water. Diglycine (5 mmol) was dissolved in 6 mL of 1 M aqueous NaOH and this solution was cooled with an ice bath. Under stirring were added simultaneously to this solution the alkanoyl chloride (10 mmol) and a 1 M aqueous NaOH solution (12 mmol). The mixture was then let to warm up to room temperature and stirred for 4 h leading to the formation of a white suspension. 1 M aqueous HCl was then added until the pH decreased to 1 and a massive precipitate was formed. The white solid was then filtered under vacuum, washed with cold water then acetone, and recrystallized (ethyl acetate / methanol, 3:1) in the case of the octyl derivative, or washed with petroleum ether in the case of the dodecyl derivative.

C$_n$-Gly-Gly-His(1-Trt)-OMe. Acylated diglycine C$_n$-Gly-Gly-OH (2.5 mmol) was placed in a flask containing Oxyma (5 mmol) and 25 mL DCM at room temperature. Addition of DIEA (1.25 mmol) led to a yellow suspension. DIC (5 mmol) was added and the mixture was maintained under stirring for an activation time of 10 min. Then a solution of H-His(1-Trt)-OMe,HCl (5 mmol) and DIEA (5 mmol) in 25 mL DCM was added to the previous mixture. The resulting solution became more limpid and was stirred for 16 h at room temperature leading to an orange solution. After removing the solvent under reduced pressure, the orange solid was dissolved in 25 mL EtOAc and this organic phase was washed successively with 25 mL of 5 % aqueous AcOH, several times with 25 mL saturated aqueous solution of NaHCO$_3$ (until the aqueous phase remained colorless), and finally twice with 25 mL brine. The organic phase was dried over Na$_2$SO$_4$, then evaporated to dryness under reduced pressure. The resulting solid was washed with 100 mL

TBME under heating. Filtration afforded the title compound as a pale yellow powder.

Cn-Gly-Gly-His-OMe. Deprotection of the trityl group was achieved using TFA in the presence of TIS and H_2O as scavengers. To C_n-Gly-Gly-His(1-Trt)-OMe (2 mmol) was added 17 mL of a 85:10:5 TFA/TIS/H_2O solution. The solid dissolved before a new precipitate formed. The mixture was stirred at 25 °C for 2 h then evaporated to dryness under reduced pressure. The resulting solid was dissolved in EtOAc (50 mL) and the organic phase was washed several times with aqueous saturated $NaHCO_3$ (100 mL) solution until the pH of the aqueous phase reached 9. During these washes, a white precipitate formed which was filtered and washed with EtOAc. Recrystallization from DCM/MeOH afforded the targeted compound.

Cn-Gly-Gly-His-OH. Cleavage of the methyl group was achieved by saponification. In a flask was placed C_n-Gly-Gly-His-OMe (2 mmol) and a solution of LiOH (3 mmol) in 20 mL of 1:1 THF/H_2O was added at 4 °C (ice bath). The suspension was stirred for 1 h at 4 °C and it was let to warm up to room temperature. Then 1 M H_2SO_4 was added until the pH value reached 3. The suspension was diluted with 30 mL H_2O and 50 mL TBME were added. After stirring, the white solid formed was collected by filtration under reduced pressure and rinsed with acetonitrile. The peptide C1 was too soluble in water and it was rather purified by desalting on a SPE column (Chromabond® HR-X/6 ml/500 mg from Macherey-Nagel).

Lipopeptides C4, C5 and C6 were synthesized according to the following general scheme (Figure 8).
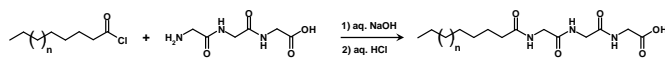
Figure 8. Synthesis of lipopeptides **C4-C6** by Schotten-Baumann acylation of triglycine

Cn-Gly-Gly-Gly-OH. Acylated triglycines were obtained by a Schotten-Baumann reaction in water. Triglycine (5 mmol) was dissolved in 6 mL of 1 M aqueous NaOH and this solution was cooled with an ice bath. Under stirring were added simultaneously to this solution the alkanoyl chloride (10 mmol) and a 1 M aqueous NaOH solution (12 mmol). The mixture was then let to warm up to room temperature and stirred for 4 h leading to the formation of a white suspension. 1 M aqueous HCl was then added until the pH decreased to 1 and a massive precipitate was formed. The white solid was then filtered under vacuum, washed with cold water then acetone and collected without further purification.

Lipopeptides N1 and N3 were synthesized according to the following general sequence depicted in Figure 9.

Boc-Gly-Gly-Cn : Protected diglycine (5.5 mmol) was placed in a flask containing Oxyma (7.5 mmol) and 20 mL of DCM at room temperature. DIC (7.5 mmol) was added and the mixture was maintained under stirring for an activation time of 10 min. The alkylamine (5 mmol) was then added to the previous mixture. The resulting solution became more limpid and was stirred for 5 h at room temperature, leading to an orange solution.
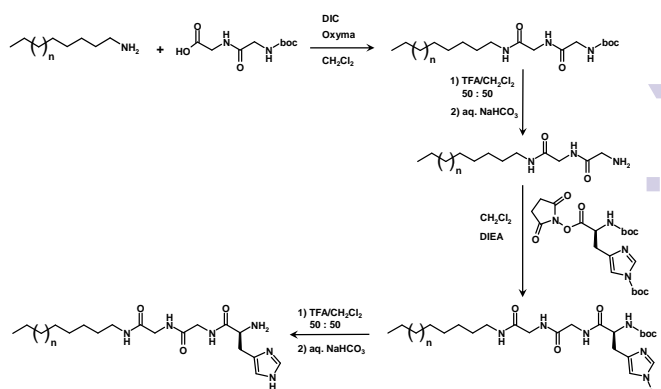
Figure 9. General synthetic pathway for the preparation of lipopeptides **N1** and **N3**.

After removing the solvent under reduced pressure, the orange solid was dissolved in 50 mL EtOAc and this organic phase was washed successively with 50 mL of 5 % aqueous AcOH, several times with 50 mL saturated aqueous solution of $NaHCO_3$ (until the aqueous phase remained colorless), and finally three times with 50 mL brine. The organic phase was dried over Na_2SO_4, then evaporated to dryness under reduced pressure. The resulting solid was washed with 100 mL petroleum ether at room temperature. Filtration afforded the title compound as a slight orange powder.

H-Gly-Gly-Cn : Protected acylated diglycine Boc-Gly-Gly-C_n (4.5 mmol) was dissolved in 10 mL of 50:50 TFA/DCM. The mixture was stirred at room temperature for 30 minutes then evaporated to dryness under reduced pressure. To the resulting solid was added aqueous saturated $NaHCO_3$ until the pH reached 8. Addition of 40 mL EtOAc (40 mL) induced the formation of a precipitate. The solid was filtered and washed twice with EtOAc, affording a beige compound.

Boc-His(1-Boc)-Gly-Gly-Cn: N-acylated diglycine H-Gly-Gly-C_n (3 mmol) was placed in a flask containing Boc-His(1-Boc)-OSu (6 mmol) and 20 mL DCM at room temperature. Addition of DIEA (9 mmol) led to a yellow suspension that was stirred for 4 h at room temperature, leading to an orange solution. After removing the solvent under reduced pressure, the orange solid was dissolved in 20 mL DCM and this organic phase was washed three times with 20 mL saturated aqueous solution of $NaHCO_3$ and twice with 20 mL water. The organic phase was dried over Na_2SO_4, then evaporated to dryness under reduced pressure. The targeted compound was obtained after recrystallization from EtOAc (octyl derivative) or after washing with petroleum ether (dodecyl derivative).

H-His-Gly-Gly-Cn: Deprotection of the two amine groups was achieved using TFA in DCM as for the deprotection of Boc-Gly-Gly-C_n. The final product was collected after preparative high performance liquid chromatography.

Lipopeptides N4, N5 and N6 were synthesized according to the following general scheme (Figure 10).
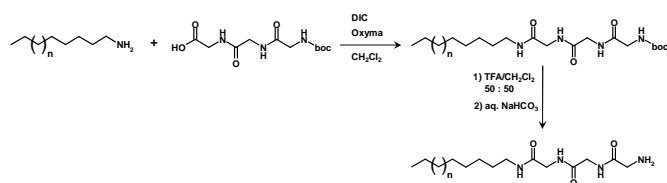
Figure 10. Two-step synthesis of lipopeptides **N4-N6** from protected triglycine.

Boc-Gly-Gly-Gly-C$_n$: Protected triglycine (4.4 mmol) was placed in a flask containing Oxyma (6 mmol) and 20 mL of DCM at room temperature. DIC (6 mmol) was added and the mixture was maintained under stirring for an activation time of 10 min. Then alkylamine (4 mmol) was added to the previous mixture. The resulting solution became more limpid and was stirred for 5 h at room temperature, leading to an orange solution. After removing the solvent under reduced pressure, the orange solid was dissolved in 50 mL EtOAc and this organic phase was washed successively with 25 mL of 5 % aqueous AcOH, several times with 25 mL saturated aqueous solution of NaHCO$_3$ (until the aqueous phase remained colorless), and finally twice with 25 mL brine. The organic phase was dried over Na$_2$SO$_4$, then evaporated to dryness under reduced pressure. During these washes, a beige precipitate formed which was filtered and washed with EtOAc.

H-Gly-Gly-Gly-C$_n$: Protected acylated triglycine Boc-Gly-Gly-Gly-C$_n$ (3.5 mmol) was dissolved in 20 mL of 50:50 TFA/DCM. The mixture was stirred at room temperature for 30 minutes then evaporated to dryness under reduced pressure. To the resulting solid was added aqueous saturated NaHCO$_3$ until the pH increased to 8 and a massive precipitate formed. The yellow solid was then filtered under vacuum, washed with water then acetone. Recrystallization from methanol/water (1:3) afforded a white compound.

C2N2: The catanionic derivative C2N2 was prepared by acid-base reaction between C$_{10}$-Gly-Gly-His-OH (C2, 0.12 mmol) and H-His-Gly-Gly-C$_{10}$ (N2, 0.12 mmol) dispersed in 60 mL water. After stirring for 2 h at room temperature, a homogeneous solution was obtained. Removal of water by freeze-drying afforded the catanionic derivative as a white powder.

Full spectroscopic characterizations and complementary analysis are reported in the *Supporting Information*.

General methods

CAC determination by surface tension measurements. Surface tension measurements were performed with a Krüss EasyDyne tensiometer using the Wilhelmy plate method. Solutions of lipopeptides were prepared by simple dissolution of the surfactants in HEPES buffer (50 mM, pH = 7, 25 °C). These stock solutions were diluted with buffer to allow covering the concentration range over few decades. For each experiment, three sets of ten readings were performed and averaged. Moreover the CAC values reported come from the averaging of several independent experiments.

CAC determination by the pyrene fluorescence method. Corrected steady state fluorescence spectra were recorded with a Photon Technology International (PTI) Quanta Master 1 spectrofluorimeter. Measurements were conducted at 25 °C in temperature-controlled quartz cells. The excitation wavelength was 337 nm and the emission spectra were recorded from 350 to 500 nm. The I$_1$/I$_3$ pyrene fluorescence ratio was calculated from the relative intensities of the emission bands at I$_1$ = 371 nm and I$_3$ = 381 nm. As for tensiometry measurements, series of lipopeptides solutions at different concentrations in HEPES buffer were prepared. For each series, a stock solution was first prepared containing a 1% *v/v* 10^{-4} M pyrene solution in methanol so that the final pyrene concentration was 10^{-6} M. Then subsequent dilutions were realized using a HEPES buffer already containing pyrene at 10^{-6} M.

Determination of the size of the aggregates by DLS. Dynamic Light Scattering (DLS) experiments were conducted at 25 °C using a ZEN 3600 Zetasizer NanoZS from Malvern, operating in backscattered mode at 173° with a 4 mW helium-neon laser (wavelength: 633 nm), with the samples placed in a thermostatted quartz cell. All measurements were carried out with regard to solvent viscosity and they were realized as triplicates. The mean sizes values obtained in the intensity distribution profiles were averaged.

Determination of the size and shape of the aggregates by SANS. Small Angle Neutron Scattering (SANS) experiments were carried out at the LLB neutron reactor facility (Leon Brillouin Laboratory at Saclay, France) at the PACE beamline. Raw data were recorded at different neutron wavelengths (13 and 6 Å) and different sample-to-detector distances (5 m and 1 m) to allow covering the entire Q-range (3·10^{-3} - 0.4 Å^{-1}). Data were then combined and finally corrected for transmission, solvent, and detector response and further normalized by 1 mm H$_2$O sample to get intensities in absolute units (cm^{-1}).

Imaging of the aggregates by TEM. The morphologies of the aggregates were evaluated by transmission electron microscopy (TEM) using a Hitachi HT7700 microscope operating at 120 kV. Specimen preparation was realized by placing a drop of the sample solution on a copper grid followed by negative staining with a 1% (w/v) sodium phosphotungstate or a 2% (w/v) uranyl acetate solution. Experiments were realized at the "Centre de Microscopie Electronique Appliquée à la Biologie" (CMEAB) platform from the Biomedical Federative Research Institute at the Rangueil Faculty of Medicine (Toulouse University).

pKa determination. Potentiometric titrations were carried out using a pH probe connected to a Model 310 pHmeter (Hanna Instruments), calibrated with standard buffers (pH = 4.01 and pH = 7.01) from Hanna Instruments. Titration were performed at 25 ± 1°C in aqueous solutions containing 0.1 M potassium chloride. Lipopeptides were prepared at 2 mM and titrated with aliquots of 0.02 M NaOH or 0.02 M HCl. Second-derivative method was chosen for pKa determination.

Kinetics experiments

For each catalysis experiment, 15 mL of a 2 mM catalyst solution was first prepared in aqueous 0.05 M HEPES buffer (pH = 7) and maintained at 25°C (± 1 °C) under stirring. The hydrolysis reaction was then initiated by adding to the catalyst 250 μL of a 1.2 M pNPA solution in acetonitrile (pNPA was not soluble enough in water). Therefore the initial concentration of pNPA was 20 mM in the reaction flask while the amount of acetonitrile remained negligible (< 2%). The reaction course was monitored spectrophotometrically at 406 nm by recording the absorbance of the pNP ion formed upon pNPA hydrolysis. Every 5 minutes, aliquots were taken and diluted at least 10 times before absorbance measurements using a Specord 600 spectrophotometer from Analytik Jena.

Notes and references

Electronic Supplementary Information (ESI) available: the *Supporting Information* includes the structural characterization of the lipopeptides, their NMR and FTIR spectra, the tensiometry and pyrene fluorescence measurements, and the determination of hydrolysis in buffer alone. See DOI: 10.1039/b000000x/

1. Bertelsen, S. and K.A. Jorgensen, *Organocatalysis-after the gold rush.* Chemical Society Reviews, 2009. **38**(8): p. 2178-2189.

2. Grondal, C., M. Jeanty, and D. Enders, *Organocatalytic cascade reactions as a new tool in total synthesis.* Nature Chemistry, 2010. **2**(3): p. 167-178.

3. Marques-Lopez, E., R.P. Herrera, and M. Christmann, *Asymmetric organocatalysis in total synthesis - a trial by fire.* Natural Product Reports, 2010. **27**(8): p. 1138-1167.

4. Moyano, A., N. El-Hamdouni, and A. Atlamsani, *Asymmetric Organocatalytic Rearrangement Reactions.* Chemistry-a European Journal, 2010. **16**(18): p. 5260-5273.

5. Zhong, C. and X.D. Shi, *When Organocatalysis Meets Transition-Metal Catalysis.* European Journal of Organic Chemistry, 2010(16): p. 2999-3025.

6. Davie, E.A.C., et al., *Asymmetric catalysis mediated by synthetic peptides.* Chemical Reviews, 2007. **107**(12): p. 5759-5812.

7. Jarvo, E.R. and S.J. Miller, *Amino acids and peptides as asymmetric organocatalysts.* Tetrahedron, 2002. **58**(13): p. 2481-2495.

8. Miller, S.J., *In search of peptide-based catalysts for asymmetric organic synthesis.* Accounts of Chemical Research, 2004. **37**(8): p. 601-610.

9. Raynal, M., et al., *Supramolecular catalysis. Part 2: artificial enzyme mimics.* Chemical Society Reviews, 2014. **43**(5): p. 1734-1787.

10. Taylor, M.S. and E.N. Jacobsen, *Asymmetric catalysis by chiral hydrogen-bond donors.* Angewandte Chemie-International Edition, 2006. **45**(10): p. 1520-1543.

11. Mase, N. and C.F. Barbas, *In water, on water, and by water: mimicking nature's aldolases with organocatalysis and water.* Organic & Biomolecular Chemistry, 2010. **8**(18): p. 4043-4050.

12. Buurma, N.J., *Kinetic medium effects on organic reactions in aqueous colloidal solutions*, in *Advances in Physical Organic Chemistry,*

Vol 43, J.P. Richard, Editor. 2009, Academic Press Ltd-Elsevier Science Ltd: London. p. 1-37.

13. Dwars, T., E. Paetzold, and G. Oehme, *Reactions in micellar systems.* Angewandte Chemie-International Edition, 2005. **44**(44): p. 7174-7199.

14. Holmberg, K., *Organic reactions in microemulsions.* European Journal of Organic Chemistry, 2007(5): p. 731-742.

15. Jongejan, M.G.M., J.E. Klijn, and J. Engberts, *Vesicular catalysis of the decarboxylation of 6-nitrobenzisoxazole-3-carboxylate. The effects of sugars, long-tailed sugars, cholesterol and alcohol additives.* Journal of Physical Organic Chemistry, 2006. **19**(4). p. 249-256.

16. Klijn, J.E. and J. Engberts, *Vesicular catalysis of an S(N)2 reaction: Toward understanding the influence of glycolipids on reactions proceeding at the interface of biological membranes.* Langmuir, 2005. **21**(22): p. 9809-9817.

17. Rathman, J.F., *Micellar catalysis.* Current Opinion in Colloid & Interface Science, 1996. **1**(4): p. 514-518.

18. Romsted, L.S. and C. Bravo-Diaz, *Modeling chemical reactivity in emulsions.* Current Opinion in Colloid & Interface Science, 2013. **18**(1): p. 3-14.

19. Romsted, L.S., C.A. Bunton, and J.H. Yao, *Micellar catalysis, a useful misnomer.* Current Opinion in Colloid & Interface Science, 1997. **2**(6): p. 622-628.

20. Dong, Z.Y., et al., *Supramolecular enzyme mimics by self-assembly.* Current Opinion in Colloid & Interface Science, 2011. **16**(6): p. 451-458.

21. Dehsorkhi, A., V. Castelletto, and I.W. Hamley, *Self-assembling amphiphilic peptides.* Journal of Peptide Science, 2014. **20**(7). p. 453-467.

22. Dejugnat, C., O. Diat, and T. Zemb, *Surfactin Self-Assembles into Direct and Reverse Aggregates in Equilibrium and Performs Selective Metal Cation Extraction.* Chemphyschem, 2011. **12**(11): p. 2138-2144.

23. Dejugnat, C. and T. Zemb, *Supramolecular assemblies formed by self-assembling peptides.* Surfactant Sci. Ser., 2011. **152**(Colloids in Biotechnology): p. 39-78.

24. Mandal, D., A.N. Shirazi, and K. Parang, *Self-assembly of peptides to nanostructures.* Organic & Biomolecular Chemistry, 2014. **12**(22): p. 3544-3561.

25. Miravet, J.F., et al., *Self-assembly of a peptide amphiphile: transition from nanotape fibrils to micelles.* Soft Matter, 2013. **9**(13): p. 3558-3564.

26. Tang, C.K., F. Qiu, and X.J. Zhao, *Molecular Design and Applications of Self-Assembling Surfactant-Like Peptides.* Journal of Nanomaterials, 2013.

27. Tsutsumi, H. and H. Mihara, *Soft materials based on designed self-assembling peptides: from design to application.* Molecular Biosystems, 2013. **9**(4): p. 609-617.

28. Zhang, S.G., *Lipid-like Self-Assembling Peptides.* Accounts of Chemical Research, 2012. **45**(12): p. 2142-2150.

29. Escuder, B., F. Rodriguez-Llansola, and J.F. Miravet, *Supramolecular gels as active media for organic reactions and catalysis.* New Journal of Chemistry, 2010. **34**(6): p. 1044-1054.

30. Rodriguez-Llansola, F., J.F. Miravet, and B. Escuder, *A supramolecular hydrogel as a reusable heterogeneous catalyst*

for the direct aldol reaction. Chemical Communications, 2009(47): p. 7303-7305.

31. Berdugo, C., J.F. Miravet, and B. Escuder, *Substrate selective catalytic molecular hydrogels: the role of the hydrophobic effect.* Chemical Communications, 2013. **49**(90): p. 10608-10610.

32. Rodriguez-Llansola, F., et al., *Structural and morphological studies of the dipeptide based L-Pro-L-Val organocatalytic gels and their rheological behaviour.* Soft Matter, 2012. **8**(34): p. 8865-8872.

33. Rodriguez-Llansola, F., J.F. Miravet, and B. Escuder, *Supramolecular Catalysis with Extended Aggregates and Gels: Inversion of Stereoselectivity Caused by Self-Assembly.* Chemistry-a European Journal, 2010. **16**(28): p. 8480-8486.

34. De Munter, S., M. Kohn, and M. Bollen, *Challenges and Opportunities in the Development of Protein Phosphatase-Directed Therapeutics.* Acs Chemical Biology, 2013. **8**(1): p. 36-45.

35. Brenner, C., *Hint, Fhit, and GalT: Function, structure, evolution, and mechanism of three branches of the histidine triad superfamily of nucleotide hydrolases and transferases.* Biochemistry, 2002. **41**(29): p. 9003-9014.

36. Anderson, J., et al., *THE HYDROLYSIS OF P-NITROPHENYL ACETATE - A VERSATILE REACTION TO STUDY ENZYME-KINETICS.* Journal of Chemical Education, 1994. **71**(8): p. 715-718.

37. Head, M.B., et al., *NUCLEOPHILIC AND ENZYMATIC CATALYSIS OF P-NITROPHENYLACETATE HYDROLYSIS.* Journal of Chemical Education, 1995. **72**(2): p. 184-186.

38. Huang, Z.P., et al., *Self-assembly of amphiphilic peptides into bio-functionalized nanotubes: a novel hydrolase model.* Journal of Materials Chemistry B, 2013. **1**(17): p. 2297-2304.

39. Hung, W.H., C.C. Hu, and C.Y. Liu, *Hydrolysis catalyzed with a resin containing histidine groups.* Journal of Molecular Catalysis a-Chemical, 1996. **106**(1-2): p. 67-73.

40. Lombardo, A., *KINETICS OF IMIDAZOLE CATALYZED ESTER HYDROLYSIS - USE OF BUFFER DILUTIONS TO DETERMINE SPONTANEOUS RATE, CATALYZED RATE, AND REACTION ORDER.* Journal of Chemical Education, 1982. **59**(10): p. 887-888.

41. Nicoll, A.J. and R.K. Allemann, *Nucleophilic and general acid catalysis at physiological pH by a designed miniature esterase.* Organic & Biomolecular Chemistry, 2004. **2**(15): p. 2175-2180.

42. Ohkubo, K., H. Ogata, and K. Yamaki, *STEREOSELECTIVE ESTEROLYSIS OF DIPEPTIDE-TYPE AMINO-ACID ESTERS WITH DI-PEPTIDE-TYPE AND TRI-PEPTIDE-TYPE L-HISTIDINE DERIVATIVES IN THE SOLUTION OF A CHIRAL CATIONIC SURFACTANT.* Journal of Molecular Catalysis, 1984. **26**(1): p. 1-5.

43. Barton, J.S., *A Comprehensive Enzyme Kinetic Exercise for Biochemistry.* Journal of Chemical Education, 2011. **88**(9): p. 1336-1339.

44. Comba, P., et al., *Monoesterase Activity of a Purple Acid Phosphatase Mimic with a Cyclam Platform.* Chemistry-a European Journal, 2012. **18**(6): p. 1700-1710.

45. Hiscock, J.R., et al., *Tripodal molecules for the promotion of phosphoester hydrolysis.* Chemical Communications, 2014. **50**(47): p. 6217-6220.

46. Lindgren, N.J.V., et al., *Downsizing of Enzymes by Chemical Methods: Arginine Mimics with Low pK(a) Values Increase the Rates of Hydrolysis of RNA Model Compounds.* Angewandte Chemie-International Edition, 2009. **48**(36): p. 6722-6725.

47. Liu, Y., et al., *Hydrolysis of phosphodiester catalyzed by metallomicelles with histidine residue: Kinetics and mechanism.* Colloids and Surfaces a-Physicochemical and Engineering Aspects, 2013. **436**: p. 839-845.

48. Merschky, M. and C. Schmuck, *Synthesis and kinetic studies of a low-molecular weight organocatalyst for phosphate hydrolysis in water.* Organic & Biomolecular Chemistry, 2009. **7**(23): p. 4895-4903.

49. Moe, O. and R. Cornelius, *ENZYME-KINETICS.* Journal of Chemical Education, 1988. **65**(2): p. 137-141.

50. Razkin, J., et al., *Enhanced complexity and catalytic efficiency in the hydrolysis of phosphate diesters by rationally designed helix-loop-helix motifs.* Chembiochem, 2008. **9**(12): p. 1975-1984.

51. Schmuck, C. and J. Dudaczek, *Screening of a combinatorial library reveals peptide-based catalysts for phosphorester cleavage in water.* Organic Letters, 2007. **9**(26): p. 5389-5392.

52. Schmuck, C., U. Michels, and J. Dudaczek, *Hydrolytic activity of histidine-containing octapeptides in water identified by quantitative screening of a combinatorial library.* Organic & Biomolecular Chemistry, 2009. **7**(21): p. 4362-4368.

53. Li, Y.S., et al., *Dipeptide seryl-histidine and related oligopeptides cleave DNA, protein, and a carboxyl ester.* Bioorganic & Medicinal Chemistry, 2000. **8**(12): p. 2675-2680.

54. Ma, Y., et al., *DNA cleavage function of seryl-histidine dipeptide and its application.* Amino Acids, 2008. **35**(2): p. 251-256.

55. Kronholm, K.G., et al., *Preparation and formulation of histidylglycylglycine and derivatives for stimulation of hair growth*, 1993, Procter and Gamble Co., USA . p. 10 pp.

56. Miyaji, N., et al., *Novel lipid-tripeptide based hydrogel-forming agent, and hydrogel*, 2009, Nissan Chemical Industries, Ltd., Japan; Kyushu University . p. 29pp.

57. Miyamoto, M., N. Miyachi, and T. Iwama, *Novel lipid dipeptide and gel prepared therefrom*, 2010, Nissan Chemical Industries, Ltd., Japan . p. 79pp.

58. Kogiso, M., Y. Zhou, and T. Shimizu, *Instant Preparation of Self-Assembled Metal-Complexed Lipid Nanotubes That Act as Templates to Produce Metal-Oxide Nanotubes.* Advanced Materials, 2007. **19**(2): p. 242-246.

59. Brady, L., et al., *A SERINE PROTEASE TRIAD FORMS THE CATALYTIC CENTER OF A TRIACYLGLYCEROL LIPASE.* Nature, 1990. **343**(6260): p. 767-770.

60. Blanzat, M., et al., *New catanionic glycolipids. 1. Synthesis, characterization, and biological activity of double-chain and gemini catanionic analogues of galactosylceramide (galactosylceramide beta(1)cer).* Langmuir, 1999. **15**(19): p. 6163-6169.

61. Subiros-Funosas, R., et al., *Oxyma: An Efficient Additive for Peptide Synthesis to Replace the Benzotriazole-Based HOBt and HOAt with a Lower Risk of Explosion(1).* Chemistry-a European Journal, 2009. **15**(37): p. 9394-9403.

62. Anastas, P. and N. Eghbali, *Green Chemistry: Principles and Practice.* Chemical Society Reviews, 2010. **39**(1): p. 301-312.

63. Sheldon, R.A., *Fundamentals of green chemistry: efficiency in reaction design.* Chemical Society Reviews, 2012. **41**(4): p. 1437-1451.

64. Simon, M.O. and C.J. Li, *Green chemistry oriented organic synthesis in water.* Chemical Society Reviews, 2012. **41**(4): p. 1415-1427.

65. Barth, A., *Infrared spectroscopy of proteins.* Biochimica Et Biophysica Acta-Bioenergetics, 2007. **1767**(9): p. 1073-1101.

66. Goormaghtigh, E., J.M. Ruysschaert, and V. Raussens, *Evaluation of the information content in infrared spectra for protein secondary structure determination.* Biophysical Journal, 2006. **90**(8): p. 2946-2957.

67. Rosen, M.J. and J.T. Kunjappu, *Surfactants and Interfacial Phenomena, Fourth Edition.* 2012: Wiley. 616 pp.

68. Aguiar, J., et al., *On the determination of the critical micelle concentration by the pyrene 1 : 3 ratio method.* Journal of Colloid and Interface Science, 2003. **258**(1): p. 116-122.

69. Gerova, M., et al., *Self-assembly properties of some chiral N-palmitoyl amino acid surfactants in aqueous solution.* Journal of Colloid and Interface Science, 2008. **319**(2): p. 526-533.

70. Estroff, L.A. and A.D. Hamilton, *Water gelation by small organic molecules.* Chemical Reviews, 2004. **104**(3): p. 1201-1217.

71. Nallet, F., *From intensity to structure of physical chemistry of disperse media.* Journal De Physique Iv, 1999. **9**(P1): p. 95-107.

72. Etienne, M.A., et al., *Beta-amyloid protein aggregation.* Methods in molecular biology (Clifton, N.J.), 2007. **386**: p. 203-25.

73. Lee, C.F., *Self-assembly of protein amyloids: A competition between amorphous and ordered aggregation.* Physical Review E, 2009. **80**(3).

74. Biggs, A.I., *A spectrophotometric determination of the dissociation constants of p-nitrophenol and papaverine.* Transactions of the Faraday Society, 1954. **50**(0): p. 800-802.

75. Akagawa, K., M. Sugiyama, and K. Kudo, *Asymmetric Michael addition of boronic acids to a [gamma]-hydroxy-[small alpha],[small beta]-unsaturated aldehyde catalyzed by resin-supported peptide.* Organic & Biomolecular Chemistry, 2012. **10**(25): p. 4839-4843.

76. Clarke, M.L. and J.A. Fuentes, *Self-Assembly of Organocatalysts: Fine-Tuning Organocatalytic Reactions.* Angewandte Chemie International Edition, 2007. **46**(6): p. 930-933.

77. Mayer, S. and B. List, *Asymmetric Counteranion-Directed Catalysis.* Angewandte Chemie International Edition, 2006. **45**(25): p. 4193-4195.

78. Miao, X., et al., *Switchable Catalytic Activity: Selenium-Containing Peptides with Redox-Controllable Self-Assembly Properties.* Angewandte Chemie International Edition, 2013. **52**(30): p. 7781-7785.

79. Trudelle, Y., *Synthesis, conformation and reactivity towards p-nitrophenyl acetate of polypeptides incorporating aspartic acid, serine and histidine.* International Journal of Peptide and Protein Research, 1982. **19**(5): p. 528-535.